

RESEARCH

Open Access



Compressive Behavior of Concrete Containing Glass Fibers and Confined with Glass FRP Composites

Djarir Yahiaoui^{*}, Mohamed Saadi and Tayeb Bouzid

Abstract

In this paper, numerous experimental tests were carried out to study the behavior of concrete containing glass fibers and confined with glass fiber-reinforced polymer (GFRP). Concrete specimens containing different fiber percentages (0.3 wt.%, 0.6 wt.%, 0.9 wt.% or 1.2 wt.%) and with different strengths of concrete (8.5 MPa, 16 MPa and 25 MPa) and different confinement levels (two, four and six layers of GFRP) were used as research parameters. The samples were tested to failure under pure axial compression. The results imply that the confinement effect with GFRP is relatively higher for concrete samples containing glass fiber (GFCC) with a percentage equal to 0.6 wt.%. The theoretical of stress ratios (f_{cc}/f_{co}) estimated by using existing ultimate strength models are found to be close to the experimental results for high strength of GFCC, but not close to the experimental results for low strength of GFCC.

Keywords: axial compression, circular columns, concrete confinement, glass FRP, FRP strengthening

1 Introduction

In the last decade, the utility of fiber-reinforced polymers (FRP), which include carbon glass FRP, carbon FRP and aramid FRP, has more advantages for rehabilitation and strengthening of current structures owing to the various benefits, excessive strength and durability, portability, the ability of fixing, quick implementation, etc. GFRPs are the most prevalent types of FRPs owing to their high strength-to-price ratio Christian and Billington (2011), Bazli et al. (2016), Feng et al. (2014), Li et al. (2016), Lam et al. (2003), Tahsiri et al. (2015).

The concrete is one among the foremost vital engineering materials within the construction field. Whereas concrete has several advantages, such as high strength, sturdy deformation resistance, and low price, it additionally presents disadvantages, such as brittleness, poor malleability

and poor crack resistance (Kizilkanat et al. (2015), Shaikh et al. (2013), Meda et al. (2016), Cromwell et al. (2011)). Students and engineers have planned the incorporation of fibers to enhance the performance of concrete. Fiber-reinforced concrete offers superior tensile strength, bending resistance, shock strength, elongation, and ductility when compared to conventional concrete. It also possesses anti-shrinkage, anti-cracking, anti-freezing, and anti-corrosion characteristics.

When the cracks are developing in fiber-reinforced concrete, the fibers bear the traction forces acting on the cracks to strengthen the concrete matrices and continue to support the traction load which stops further crack development. In the literature different types of fibers have been reported, such as steel fibers, polypropylene fibers, carbon fibers, glass fibers, basalt fibers, polyvinyl alcohol fibers, and mixed fibers (Chao et al., 2009; Xie et al., 2019; Zhu et al., 2019; Feng et al., 2019; Sun et al., 2019; Signorini et al., 2020; Liu et al., 2020; Mohammad Hosseini et al. 2020). The addition of 0.5% to 1.5% steel fibers by fiber volume was found to augment the traction strength of concrete by 37–177% (Wang et al., 2019).

Journal information: ISSN 1976-0485 / eISSN 2234-1315

*Correspondence: d.yahiaoui@univ-batna2.dz

LGC-ROI, Civil Engineering Laboratory-Risks and Structures in Interactions,
Department of Civil Engineering, Faculty of Technology, University of Batna 2,
5000 Batna, Algeria



© The Author(s) 2022. **Open Access** This article is licensed under a Creative Commons Attribution 4.0 International License, which permits use, sharing, adaptation, distribution and reproduction in any medium or format, as long as you give appropriate credit to the original author(s) and the source, provide a link to the Creative Commons licence, and indicate if changes were made. The images or other third party material in this article are included in the article's Creative Commons licence, unless indicated otherwise in a credit line to the material. If material is not included in the article's Creative Commons licence and your intended use is not permitted by statutory regulation or exceeds the permitted use, you will need to obtain permission directly from the copyright holder. To view a copy of this licence, visit <http://creativecommons.org/licenses/by/4.0/>.

The fiber volume increased and it was observed that the tensile and compressive strengths first increased and then decreased. In addition, fibers 6 mm long were found to be better than fibers 12 mm long. Therefore, differing kinds and lengths of fibers have different effects. Furthermore, small flexible fibers have been observed to be better suitable for controlling the formation of micro-cracks while large and stiff fibers have been proven to be more suitable for controlling the development of cracks (Ganesan et al., 2014).

Therefore, the use of a combination of different fibers can lead to certain synergistic effects. For example, the combined use of polyvinyl alcohol fibers and steel fibers help to achieve optimal tensile behavior (Liu et al., 2020). It was also shown that adding a sufficient amount of basalt fibers reduced the porosity of the concrete and thus improved its durability (Guo et al., 2019; Niu et al., 2020).

However, compressive resistance does not always increase with the percentage of GFRP in concrete, implying that there is an ideal content of GFRP in concrete in order to obtain maximum compressive strength (Di Zheng et al., 2020). For the experiments, a series of concrete specimens with varying percentages of fiber 0 wt.%, 0.4 wt.%, 0.8 wt.%, or 1.2 wt.% were employed. The experimental data reveal that the uniaxial compressive strength of fiber concrete (FRC) initially increased with 0.8 wt.% and subsequently decreased with increasing fiber dose. The optimum glass fiber content is determined by the fiber type. In principle, shorter gfs with higher length–diameter ratios are more successful at regulating the formation of tiny cracks, whereas longer gfs with lower length–diameter ratios are more effective at controlling the development of micro-cracks (Kasagani and Rao 2018).

In contrast, the lateral limiting stress furnished with the aid of using wrapped FRP jacket will increase constantly with lateral evolution because of the linear elastic conduct of FRP. As a result, this sort of lateral inclusion modifies the compression conduct of regular concrete and results in compression hardening conduct (Mirmiran & Shahawy, 1997; Spoelstra & Monti, 1999). It is hypothesized that the inclusion-induced compressive strain of FRP are also applicable to glass fiber-containing concrete.

The combination of glass fiber-containing concrete (GFCC) wrapped with an FRP jacket can improve the overall performance of concrete. Thus, the unique combined properties in compression and tension of FRP-confined GFCC have great potential to optimize and improve the performance of structural components. It is necessary to prove this hypothesis experimentally and to

observe the interactions among FRP and GFCC in such configurations.

The originality of this study consists in the evaluation of the effect of wrapped FRP jacket of concrete containing different percentages of glass fibers on strength properties and failure mechanism of fiber-reinforced concrete, and the axial strength versus strain responses of GFCC cylinders externally confined with GFRPs. Another goal of this study is to evaluate the applicability of the strength force models (which are mainly developed for special FRPs) at GFR–GFCC. For this purpose, 48 GFCC cylinders were created and tested under monotonous axial compression. The research parameters included the concrete strength (such as 25 MPa, 16 MPa and 8.5 MPa), the fiber percentages (0 wt.%, 0.3 wt.%, 0.6 wt.%, 0.9 wt.%, 1.2 wt.%) and the layers of the GFRP (2 layers, 4 layers, 6 layers).

2 Test Program

In order to evaluate the feasibility of this new composite material, the behavior of glass fiber-containing concrete (GFCC), which is by glass fiber-reinforced polymer (GFRP) composites, was investigated under axial compression. For this aim, 48 round concrete columns were built and examined; the diameter and height of the concrete columns were 150 mm and 300 mm, respectively, Fig. 1. The test programmer is summarized in Table 1. It is divided into four groups according to the type of concrete strength, the number of layers of glass-GRP composite materials and the proportion of reinforcing fibers contained in the concrete.

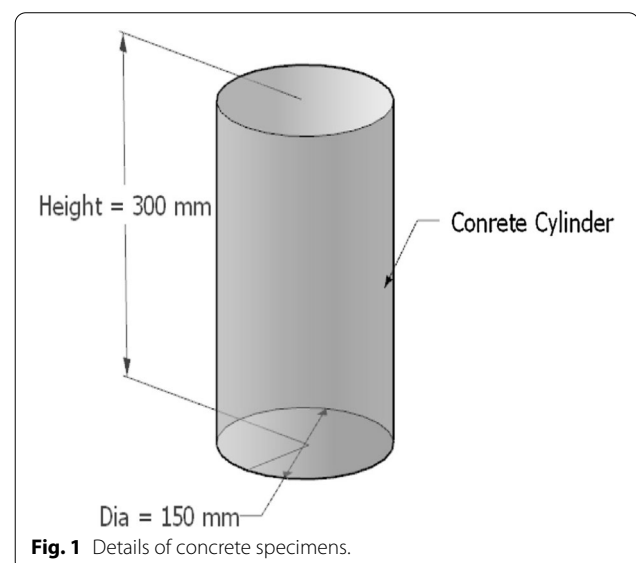


Fig. 1 Details of concrete specimens.

Table 1 Details of circular concrete cylinders.

Test cylinders	Design strength of concrete (MPa)	Volume fraction of concrete V_f (%)	GFRP thickness (layers)
S8.5-F0.3-NL0	8.5	0.3%	0
S8.5-F0.3-NL2	8.5	0.3%	2
S8.5-F0.3-NL4	8.5	0.3%	4
S8.5-F0.3-NL6	8.5	0.3%	6
S8.5-F0.6-NL0	8.5	0.6%	0
S8.5-F0.6-NL2	8.5	0.6%	2
S8.5-F0.6-NL4	8.5	0.6%	4
S8.5-F0.6-NL6	8.5	0.6%	6
S8.5-F0.9-NL0	8.5	0.9%	0
S8.5-F0.9-NL2	8.5	0.9%	2
S8.5-F0.9-NL4	8.5	0.9%	4
S8.5-F0.9-NL6	8.5	0.9%	6
S8.5-F1.2-NL0	8.5	1.2%	0
S8.5-F1.2-NL2	8.5	1.2%	2
S8.5-F1.2-NL4	8.5	1.2%	4
S8.5-F1.2-NL6	8.5	1.2%	6
S16-F0.3-NL0	16	0.3%	0
S16-F0.3-NL2	16	0.3%	2
S16-F0.3-NL4	16	0.3%	4
S16-F0.3-NL6	16	0.3%	6
S16-F0.6-NL0	16	0.6%	0
S16-F0.6-NL2	16	0.6%	2
S16-F0.6-NL4	16	0.6%	4
S16-F0.6-NL6	16	0.6%	6
S16-F0.9-NL0	16	0.9%	0
S16-F0.9-NL2	16	0.9%	2
S16-F0.9-NL4	16	0.9%	4
S16-F0.9-NL6	16	0.9%	6
S16-F1.2-NL0	16	1.2%	0
S16-F1.2-NL2	16	1.2%	2
S16-F1.2-NL4	16	1.2%	4
S16-F1.2-NL6	16	1.2%	6
S25-F0.3-NL0	25	0.3%	0
S25-F0.3-NL2	25	0.3%	2
S25-F0.3-NL4	25	0.3%	4
S25-F0.3-NL6	25	0.3%	6
S25-F0.6-NL0	25	0.6%	0
S25-F0.6-NL2	25	0.6%	2
S25-F0.6-NL4	25	0.6%	4
S25-F0.6-NL6	25	0.6%	6
S25-F0.9-NL0	25	0.9%	0
S25-F0.9-NL2	25	0.9%	2
S25-F0.9-NL4	25	0.9%	4
S25-F0.9-NL6	25	0.9%	6
S25-F1.2-NL0	25	1.2%	0
S25-F1.2-NL2	25	1.2%	2
S25-F1.2-NL4	25	1.2%	4
S25-F1.2-NL6	25	1.2%	6

3 Material Properties

Type I general purpose Portland cement was used as the binder in this research. Physical and chemical properties of this binder are provided in Table 2.

4 Glass Fiber—Alkali-Resistant

Alkali-resistant chopped strands of high tensile-strength GFRP were used as the fiber reinforcement; the overview and properties of GFRP are shown in Table 3. Four groups of mixed concrete were produced containing alkali-resistant fiber strengthened with percentages 0 wt.%, 0.3 wt.%, 0.6 wt.%, 0.9 wt.%, 1.2 wt.%, respectively, as by volume replacement of natural coarse aggregate; see Table 3.

5 Glass Fiber-Reinforced Polymer

Locally available bi-directional fiber glass (Fig. 2) and polyester resin were used to develop a low-cost glass fiber-reinforced polymer (GFRP) composite. This type of bi-directional fiber glass is widely used in the boating industry. The behavior of the GFRP composites was determined. Using the standard tensile coupon test, tensile coupons were made using various layers of fiber glass, such as one, two, three, four, and five layers to obtain accurate results. In addition, three tensile specimens were tested for each thickness to get average results.

The tensile specimens were tested using the UTS-SHIMADZU universal testing machine according to the standard guidelines of the ASTM D638 (1990), see Table 4.

Specimens are placed in the grips of a Universal Test Machine at a specified grip separation and pulled until failure. For ASTM D638 the test speed can be determined by the material specification or time to failure (1–10 min). A typical test speed for standard test specimens is 2 mm/min (0.05 in/min).

6 Preparation of Test Specimens

First gravel, sand, water and cement were weighed on an electronic scale. The fiber is light in weight and easily floats on the liquid surface. The cement, sand, gravel and fiber were added with a suitable amount of water until the fibers were sufficiently dispersed, and the prepared suspension was poured into prepared molds for tap molding.

Second, the GFRP composites were applied after 28 days. The concrete surface was properly cleaned to remove dust prior to the application of the GFRP compound. In the first step, the polyester resin was applied to the concrete surface with a brush and then a resin-soaked fiber glass board was wrapped around

Table 2 Mixture proportions of concrete

Material	Mix# 1 (8.5 MPa)	Mix# 2 (16 MPa)	Mix# 3 (25 MPa)
Cement	200 kg/m ³	300 kg/m ³	400 kg/m ³
Sand	853 kg/m ³	810 kg/m ³	773 kg/m ³
Coarse aggregate	853 kg/m ³	520 kg/m ³	496 kg/m ³
Fine aggregate	481 kg/m ³	520 kg/m ³	496 kg/m ³
Water	100 kg/m ³	132 kg/m ³	163 kg/m ³
Superplasticizer	As required	As required	As required
Compressive strength MPa	8.5	16	25

Table 3 Properties of fiber reinforcement.

Material	Length (mm)	Filament diameter (mm)	Tensile strength (MPa)	Elastic modulus (MPa)	Density (kg/m ³)	Picture
Glass fiber—alkali-resistant	3–4.5	0.015	1500–1700	72,000	2600	

the circular concrete cylinder. The typical process of GFRP strengthening is shown in Fig. 3a, b and the final strengthened specimen is displayed in Fig. 3c.

7 Instrumentation and Test Setup

Detailed instrumentation for accurate recording and control of the lateral dilation and axial strain of the GFRP-confined GFCC cylinders was used. Compressive strength tests were carried out to evaluate the strength properties of GFRP-confined GFCC cylinders using a testing machine with a capacity of 2000 KN. A total of the three LVDTs were mounted in a steel frame which was specially developed for the concrete cylinders with threaded bolts. In addition, strain gauges were installed horizontally in the GFRP mixture at mid-height of the concrete cylinders in order to record the lateral expansion and tension of FRP (Fig. 4). The specimens were loaded under compressing at a constant stroke rate of 0.1 kN/s.

8 Experimental Results

8.1 Ultimate Failure Modes

Fig. 5 represents the crack propagation pattern and failure mode of GFCC (concrete containing different fiber percentages (0.3 wt.%, 0.6 wt.%, 0.9 wt.% or 1.2 wt.%))

for three types of strength of concrete (25 MPa, 16 MPa, 8.5 MPa). In the literature, the failure patterns of ordinary concrete are a sudden collapse after the peak load and are loudly destructive, due to the crushing and splitting of concrete at the middle location. The presence of glass fiber (GF) in the concrete matrix stopped complete crushing of specimens. The increase in GF percentage led to an increase in the stability of concrete at failure (Fig. 5). The longitudinal failure pattern and fracture surface observed for samples and not showed diagonal cone type failures. Upon compression, the interfacial bonds among the GF and the cement paste could rupture, due to the bad the interfacial transition, inflicting void generation, and consequently, ease of failure.

Figs. 6, 7 and 8 show the typical failure modes of test cylinders of GFCC with different strengths of concrete (25 MPa, 16 MPa, 8.5 MPa) and confined with two, four and six layers of GFRP. In the literature, the ultimate failure modes of ordinary concrete confined with GFRP are at the mid-height of the concrete cylinders, whereas in the case of GFRP-confined GFCC the ultimate failure modes were longitudinal and mid-height of the concrete cylinders. The longitudinal strain is due to the tensile strength of the GFCC and the lateral strain in the middle of the specimen is due to the tensile strength of the

Table 4 Mechanical properties of epoxy resin and GFRP composite.

FRP composite	Tensile stress (MPa)	Ultimate strain (%)	Modulus of elasticity (Gpa)	Standard deviation
Epoxy resin	17.20	0.6322	2.72	1.08
GFRP	377.64	2.04%	18.70	1.91



Fig. 2 Bi-directional glass fiber.

LC-FRP. The phenomenon of debonding the G-FRP layer has also been observed, especially in low-strength concrete. The debonding may be attributed to the entrapped air while coating and wrapping which may weaken the confinement effect (Table 4).

8.2 Stress Versus Strain Relationships

Table 5 summarizes the experimental results of ultimate axial stress, strain and ultimate strain. The responses of axial stress–strain are displayed in Figs. 9, 10 and 11.

It can be seen that all the curves are monotonically ascending in both the first segment and the second segment followed by a sudden drop in stress; whereas, the compressive failure of GFCC is characterized by a compression softening behavior.

The axial stress versus strain responses of GFCC specimens indicate that the stress is affected by the addition of GF in the concrete. For concrete strengths equal to 25 MPa, 16 MPa and 8.5 MPa the compression increased by (26%, 32%, 30%, 10%), (25%, 31%, 25%, 11%) and (20%, 29%, 24%, 10%) for the percentage of 0.3 wt.%, 0.6 wt.%, 0.9 wt.% and 1.2 wt.%, respectively. Through these observations, we find that the samples of GFCC containing 6 wt.% of FRP gave higher values of stress and strain than all the other samples.

Through Figs. 9, 10 and 11, it can be seen that GFRP-confined GFCC is very efficient and both the ultimate stress and ultimate strains are higher than the unreinforced specimens. The stiffness of GFRP-confined GFCC is found to be higher than the GFCC not confined. The curve of axial stress–strain of GFRP-confined GFCC consists of two slanted lines. The first slope follows the trend of the control sample linearly and the second slope is also linear up to the tensile failure of the GRP compound. However, the stiffness of the second line is much lower than the first line of the axial stress–strain curve. A region of transition is observed between the first



Fig. 3 A, B Application of resin on the concrete and glass fiber wrapping, and C typical GFRP strengthened specimens.

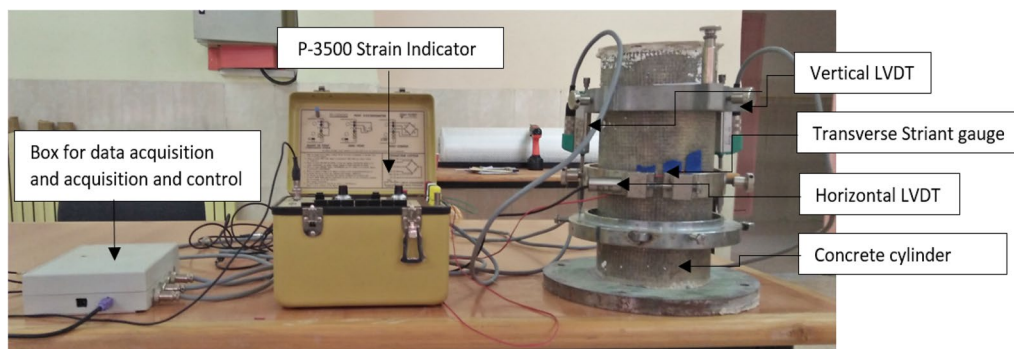


Fig. 4 Experimental setup and data acquisition system for compression concrete testing of a concrete cylinder specimen.

line and second line, which is mainly due to the stress transfer from the ARGF-reinforced concretes to the GFRP composites.

8.3 Effect of GFRP Layers

In this study, three different confinement levels, i.e., two, four, and six layers of GFRP composites were considered to examine the effect of confinement level on overall responses of GFRP-confined GFCC. The impact of confinement on axial strength, axial strain, and lateral strain is shown in Figs. 9, 10 and 11 for concrete strengths 8.5 MPa, 16 MPa and 25 MPa, respectively. The results indicate that the degree of confinement had a positive effect on the axial strength and lateral strain responses for different levels of concrete strength with an increase in the confinement level.

For example, the axial strength of GFCC specimens which were confined with two, four and six layers of GFRP was found to be between 20 and 25% for two layers, 60% and 75% for four layers and 90% and 110% for six layers, higher than the reference specimen of mixture containing 0.3%, 0.6%, 0.9% and 1.2%, respectively. The axial strains of GFCC specimens which were confined with two, four and six layers of GFRP were found to be between 372 and 590% for strength concrete 25 MPa, 217% and 1113% for strength concrete 16 MPa, and between 217 and 1113% for strength concrete 8.5 MPa, higher than the reference specimen of mixture containing 0.3%, 0.6%, 0.9% and 1.2%. The lateral strains of these specimens were found to be between 542 and 988% for strength concrete 25 MPa, 340% and 1619% for strength concrete 16 MPa, and between 227 and 1607% for strength concrete 8.5 MPa, higher than the reference specimen of mixture containing 0.3%, 0.6%, 0.9% and 1.2%.

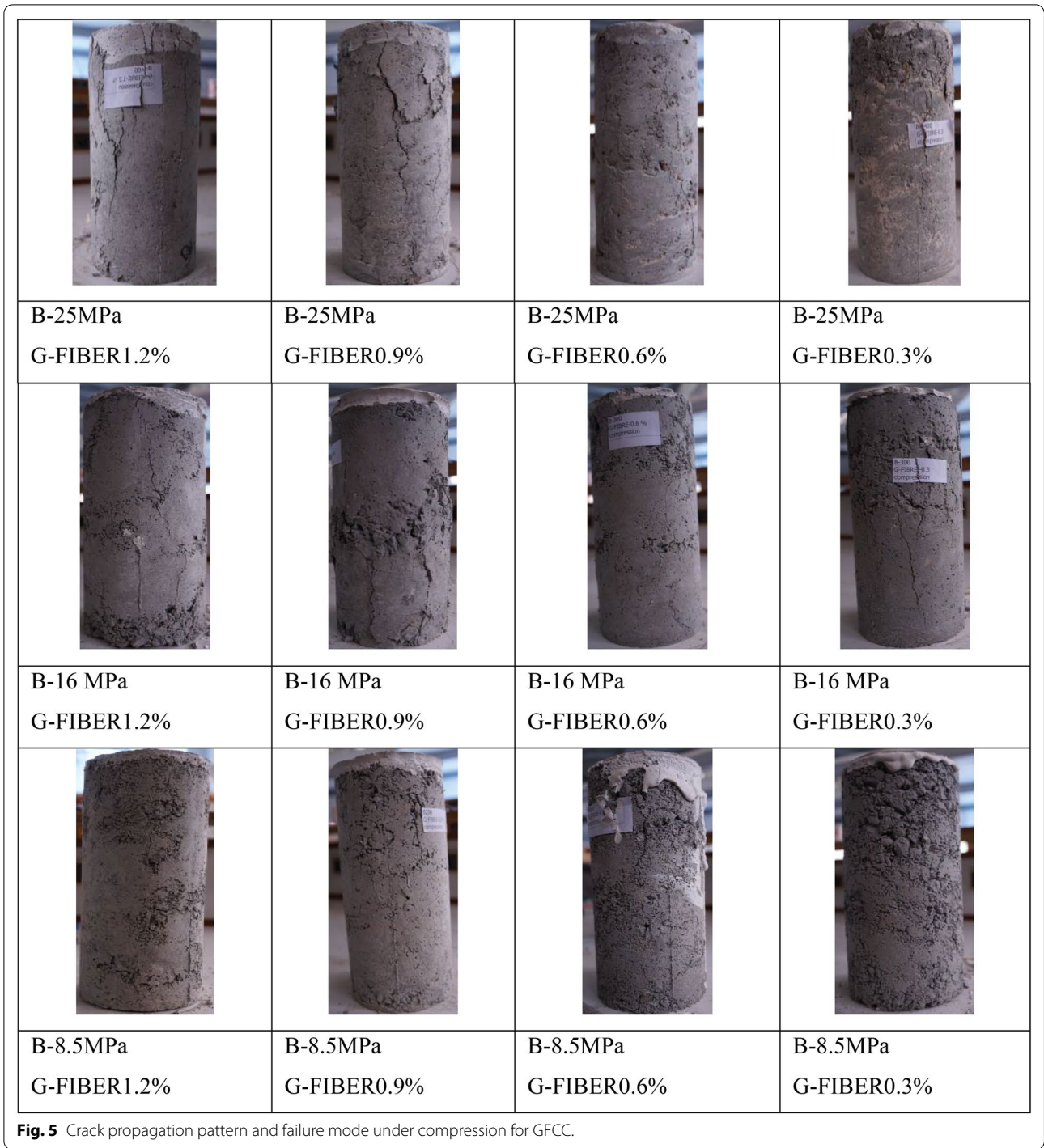
It can be seen that the thickness of the FRP was mainly not affect the transition point, but it affects the second linear sections of the curves. The dilation of GFCC was signified by the development of cracks, the axial stress–strain curves of specimens with a thicker FRP tended to have a better confinement effect on the development of cracks and thus a longer transition segment of the stress–strain curves.

9 Analytical Investigation

Various models have been proposed in literature studies to theoretically represent the ultimate strength and strain [35–37]. Table 6 contains a list of selected models for different types of FRP compounds with different inclusion coefficients. The comparison between the estimated and experimental values is shown in Figs. 12, 13.

Fig. 12 shows the comparison between the theoretical models and experimental results of ultimate strength. It can be seen that the prediction accuracy on the ultimate strengths of concrete between the results of theoretical models and experiments are affected by the strengths of concrete. For example for concrete strength equal to 25 MPa, all models are very close to the experimental results of GFRP-confined GFCC groups. But for concrete strength equal to 16 MPa the predicted accuracies are an average estimate, and for concrete strength equal to 8.5 MPa are an overestimate.

The results indicate that the augmentation in the difference between the design strength and the experimental strength are due to the increase in in concrete strength. For concrete strength equal to 25 MPa the diffre nec are slightly higher of 8% ,5%,3% and 2% for models Gher-nouti et al. (2011), Bensaid et al. (2010), AL-Salloum et al. (2007) and Teng et al. (2007) respectively. And for





			
G-FIBER 1.2% 2-Layers	G-FIBER 0.9% 2-Layers	G-FIBER 0.6% 2-Layers	G-FIBER 0.3% 2-Layers
			
G-FIBER 1.2% 4-Layers	G-FIBER 0.9% 4-Layers	G-FIBER 0.6% 4-Layers	G-FIBER 0.3% 4-Layers
			
G-FIBER 1.2% 6-Layers	G-FIBER 0.9% 6-Layers	G-FIBER 0.6% 6-Layers	G-FIBER 0.3% 6-Layers

Fig. 7 Typical failure modes of test cylinders (strength concrete = 16 MPa).



concrete strength equal to 16 MPa, The results indicate an increase in 13% ,18%,20% and 20% for models Ghernouti et al. (2011), Bensaid et al. (2010), AL-Salloum et al. (2007) and Teng et al. (2007) respectively. For concrete strength equal to 8.5 MPa, The results indicate an increase in 54% ,60%,65% and 70% for models Ghernouti et al. (2011), Bensaid et al. (2010), AL-Salloum et al. (2007) and Teng et al. (2007) respectively. Although the

theoretical predictions of the current models are close to the experimental results of high-strength concrete, there is still a need to develop more accurate strength models for low strength of GFRP-confined GFCC.

Fig. 13 shows the comparison between the theoretical models and experimental results of ultimate strain. The estimated values of ultimate strain models proposed by Teng et al. (2007) are quite close to the

Table 5 Summary of test results.

Group	Specimen	Number Layers	Axial strength (Mpa)		Axial Strain		Lateral Strain					
			f'_c	f'_{cc}	ϵ'_c	ϵ'_{cc}	ϵ'_{ch}	ϵ'_{cch}	f'_{cc}/f'_c	$\epsilon'_{cc}/\epsilon'_c$	$\epsilon'_{cch}/\epsilon'_{ch}$	
1	S25-F0.3	0	31.6		0.0029		0.0026					
		2		39.9		0.014		0.019	1.26	4.72	7.42	
		4		51.28		0.020		0.022	1.62	6.92	8.38	
		6		61.5		0.020		0.022	1.95	6.91	8.42	
	S25-F0.6	0	33.01		0.004		0.0027					
		2		42.5		0.018		0.024	1.29	4.48	9.04	
		4		56.11		0.019		0.019	1.70	4.73	6.96	
	S25-F0.9	6		66.02		0.023		0.021	2.00	5.70	7.70	
		0	32.74		0.0038		0.00317					
		2		39.73		0.016		0.025	1.21	4.08	7.98	
	S25-F1.2	4		56.57		0.019		0.035	1.73	4.95	10.88	
		6		65.49		0.024		0.030	2.00	6.37	9.53	
		0	27.5		0.00309		0.00248					
	S25-F1.2	2		36.24		0.014		0.019	1.32	4.53	7.74	
		4		46.75		0.019		0.026	1.70	6.15	10.52	
		6		55.01		0.021		0.017	2.00	6.67	7.02	
	2	S16-F0.3	0	20.69		0.0025		0.002				
			2		26.18		0.014		0.013	1.27	5.60	6.45
4				32.93		0.018		0.016	1.59	7.04	8.05	
6				39.36		0.027		0.021	1.90	10.96	10.50	
S16-F0.6		0	21.12		0.0034		0.0021					
		2		26.88		0.011		0.020	1.27	3.18	9.33	
		4		35.7		0.019		0.027	1.69	5.59	12.81	
S16-F0.9		6		42.1		0.021		0.036	1.99	6.18	17.19	
		0	20.48		0.0019		0.003					
		2		25.7		0.009		0.013	1.25	4.78	4.40	
S16-F1.2		4		32.13		0.020		0.015	1.57	10.68	5.10	
		6		41.41		0.027		0.025	2.02	14.21	8.17	
		0	17.9		0.0022		0.002					
S16-F1.2		2		22.6		0.015		0.011	1.26	6.73	5.60	
		4		29.2		0.019		0.014	1.63	8.55	6.95	
		0	10.25		0.0047		0.0018					
3		S8.5-F0.3	2		13.45		0.022		0.016	1.31	4.57	8.89
			4		17.76		0.025		0.012	1.73	5.21	6.67
	6			21.77		0.031		0.022	2.12	6.66	12.22	
	0		11.68		0.0022		0.0015					
	S8.5-F0.6	2		14.7		0.014		0.026	1.26	6.18	17.07	
		4		19.21		0.018		0.014	1.64	8.00	9.33	
		6		22.6		0.021		0.010	1.93	9.55	6.87	
	S8.5-F0.9	0	10.68		0.0037		0.0029					
		2		13.85		0.014		0.011	1.30	3.73	3.72	
		4		17.29		0.019		0.013	1.62	5.14	4.48	
	S8.5-F1.2	6		23.91		0.030		0.035	2.24	8.19	12.07	
		0	9.35		0.0029		0.0018					
		2		12.5		0.023		0.013	1.34	8.07	7.22	
	S8.5-F1.2	4		16.89		0.030		0.012	1.81	10.28	6.67	
		6		18.7		0.036		0.010	2.00	12.31	5.61	

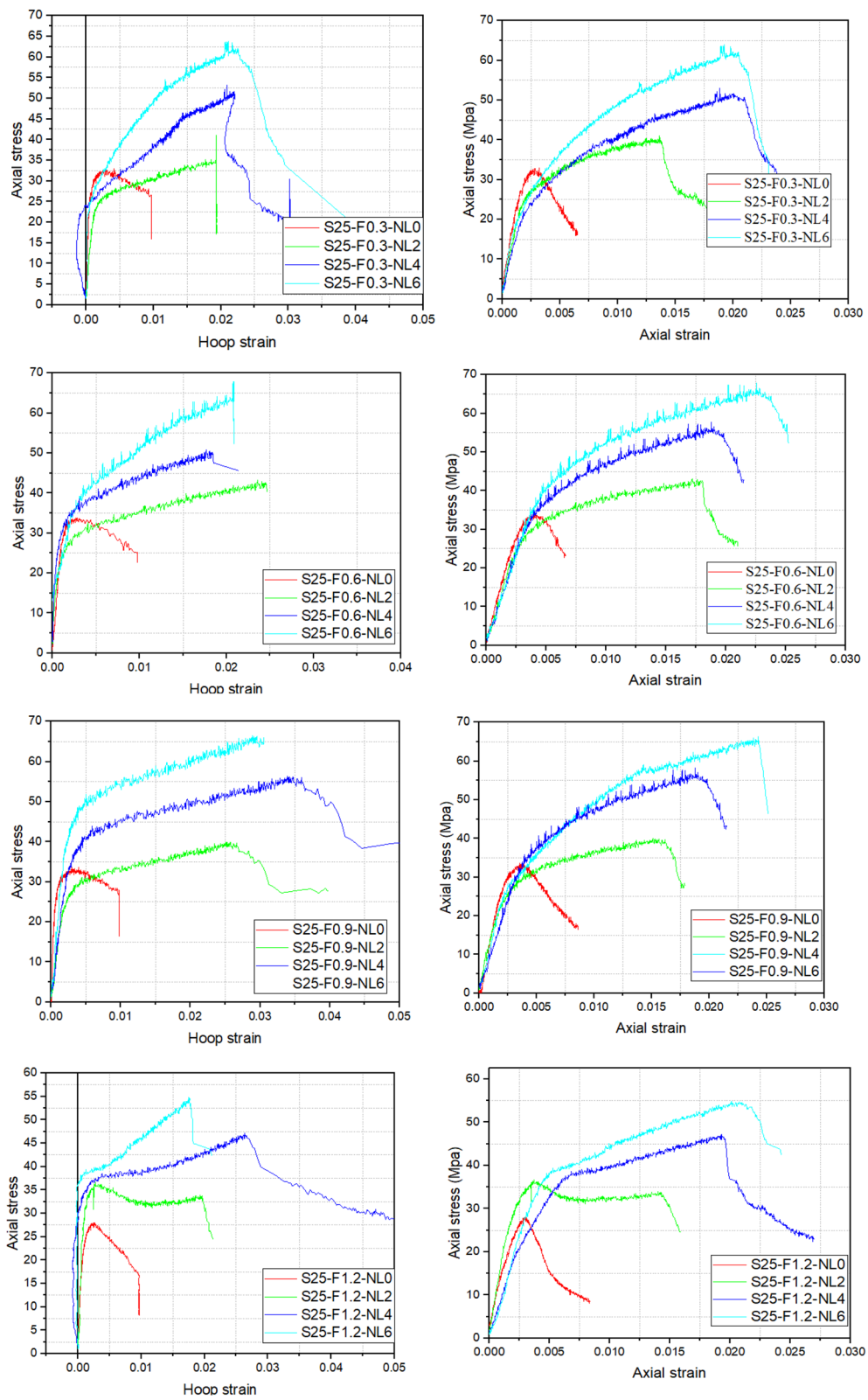


Fig. 9 Stress versus strain responses (25Mpa).

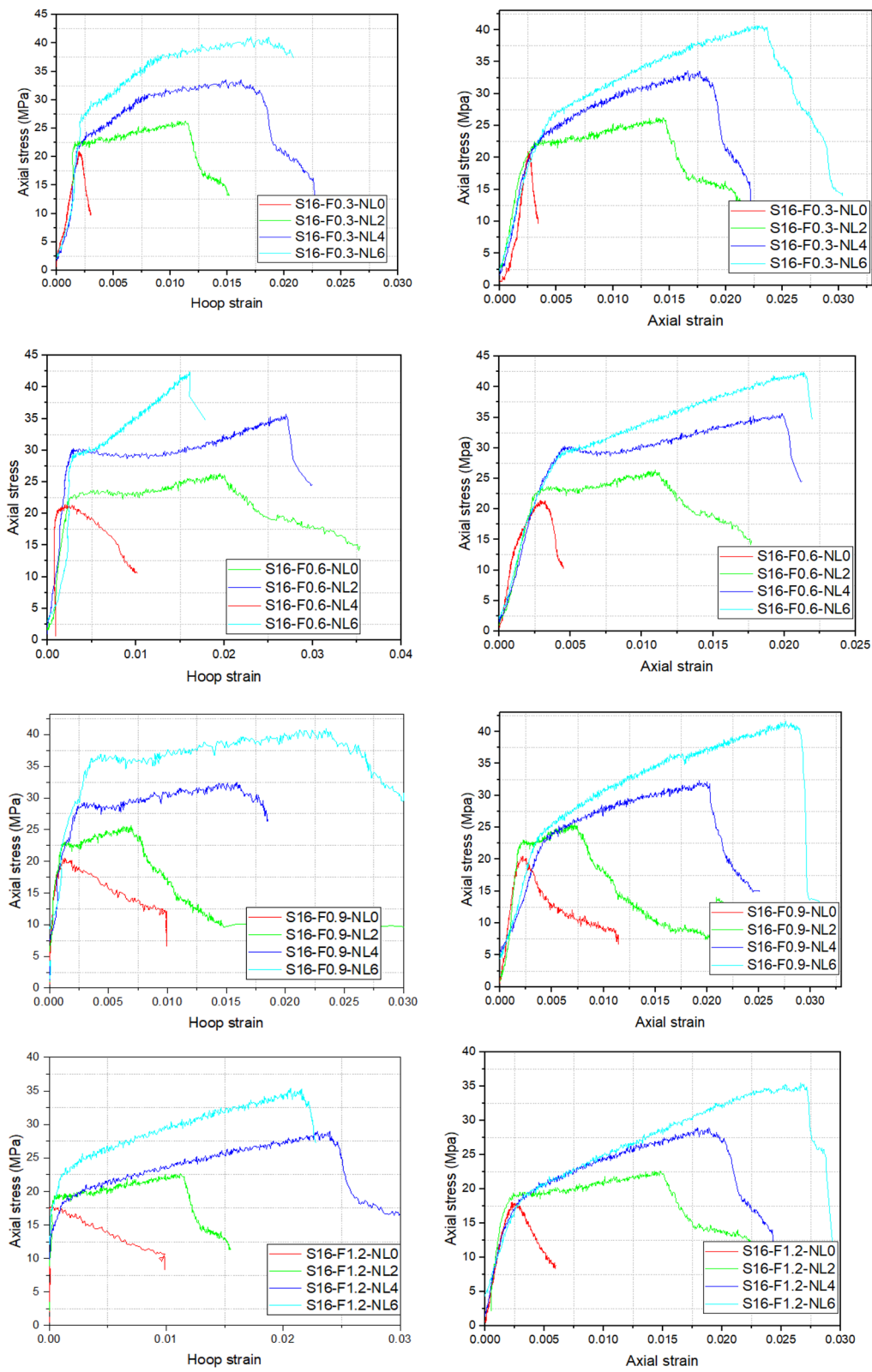


Fig. 10 Stress versus strain responses (16Mpa).

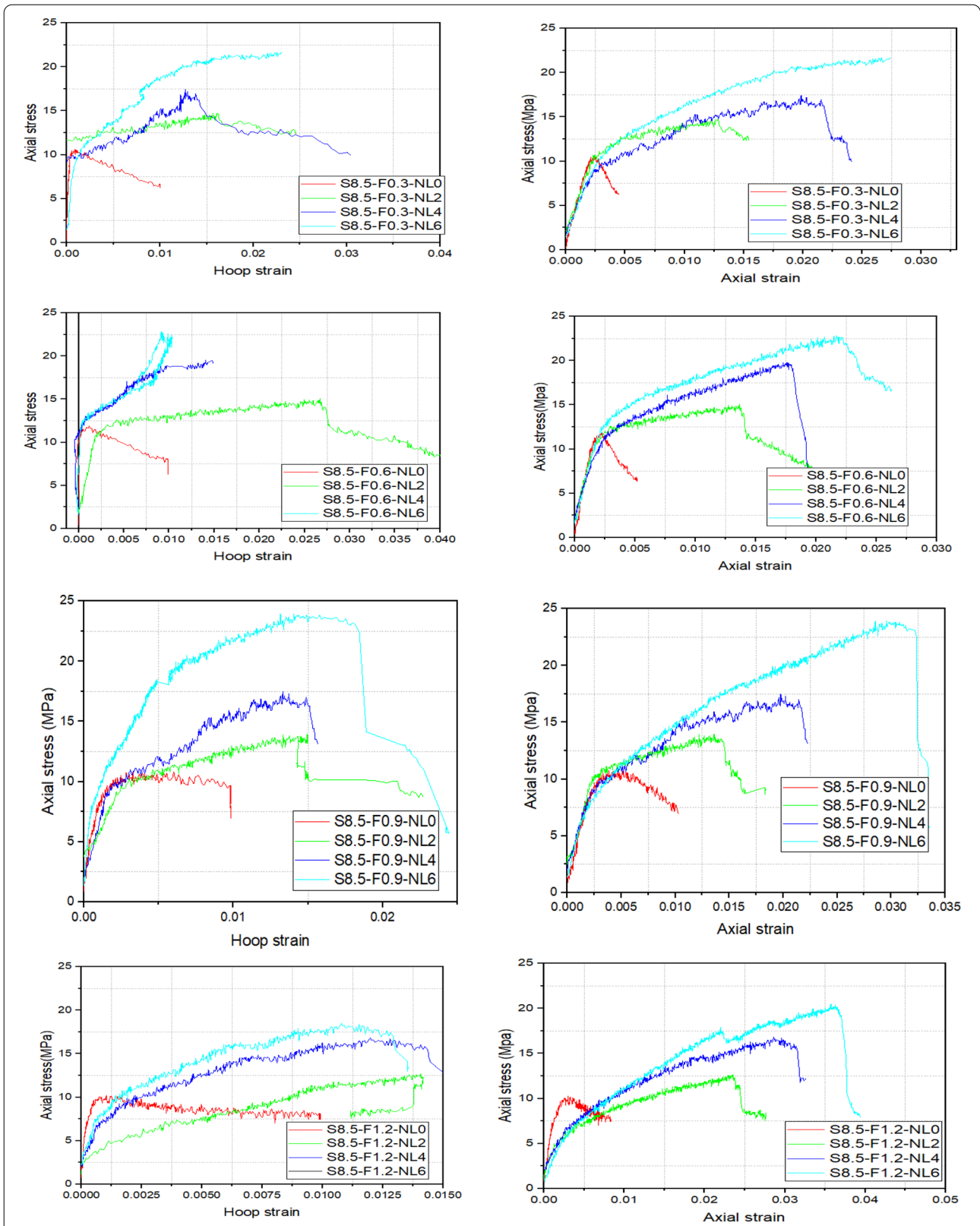


Fig. 11 Stress versus strain responses (8.5Mpa).

Table 6 Ultimate strength models.

Model	Ultimate stress	Ultimate strain
Ghernouti et al. (2011)	$f_{cc} = \left[1 + 2.023 \left(\frac{f_l}{f_{co}} \right) \right] f_{co}$	$\epsilon_{cc} = \left[1 + 10.63 \left(\frac{f_l}{f_{co}} \right) \right] \epsilon_{co}$
Benzaid et al (2010)	$f_{cc} = \left[1 + 2.20 \left(\frac{f_l}{f_{co}} \right) \right] f_{co}$	$\epsilon_{cc} = \left[1 + 7.60 \left(\frac{f_l}{f_{co}} \right) \right] \epsilon_{co}$
Al-Salloum (2007)	$f_{cc} = \left[1 + 2.312 \left(\frac{f_l}{f_{co}} \right) \right] f_{co}$	$\epsilon_{cc} = \left[1 + 0.024 \left(\frac{f_l}{f_{co}} \right) \right] \epsilon_{co}$
Bisby et al (2005)	$f_{cc} = \left[1 + 2.425 \left(\frac{f_l}{f_{co}} \right) \right] f_{co}^{-}$	
Teng et al (2007)	$f_{cc} = \left[1 + 3.5 \left(\frac{f_l}{f_{co}} \right) \right] f_{co}$	$\epsilon_{cc} = \left[1 + 17.50 \left(\frac{f_l}{f_{co}} \right) \right] \epsilon_{co}$

f_{co} =un-confined stress (MPa), f_{cc} =ultimate stress (MPa), f_l =confining pressure (MPa)

experimental results of strength of GFRP-confined GFCC equal to 25 MPa and 16 MPa. However, the theoretical predictions of Ghernouti et al. (2011), Benzaid et al. (2010) and Al-Salloum et al. (2007) are not accurate for predicting the ultimate strain, so there is still a need to develop more accurate strain models for low strength of GFRP-confined GFCC.

10 Conclusions

This paper investigates the confinement effects of glass fiber-reinforced polymer composites on circular concrete columns made with concrete contained GF. Three types of strength of concrete locally available (8.5 Mpa, 16 Mpa and 25 Mpa) were confined with GFRP. In this study, a total number of 48 circular concrete columns were constructed and tested under monotonic axial compression. Based on experimental and analytical investigations, a few conclusions are summarized below:

- The combination of GFCC wrapped with a GFRP jacket has a beneficial effect on the lateral strain.
- The response of GFCC specimens after ultimate stress is characterized by a compression softening behavior; whereas, the axial stress-strain responses of GFRP-confined specimens essentially comprised bilinear behavior.
- The effect of the number of layers GFRP composite shows a positive behavior on the ultimate stress and strain.

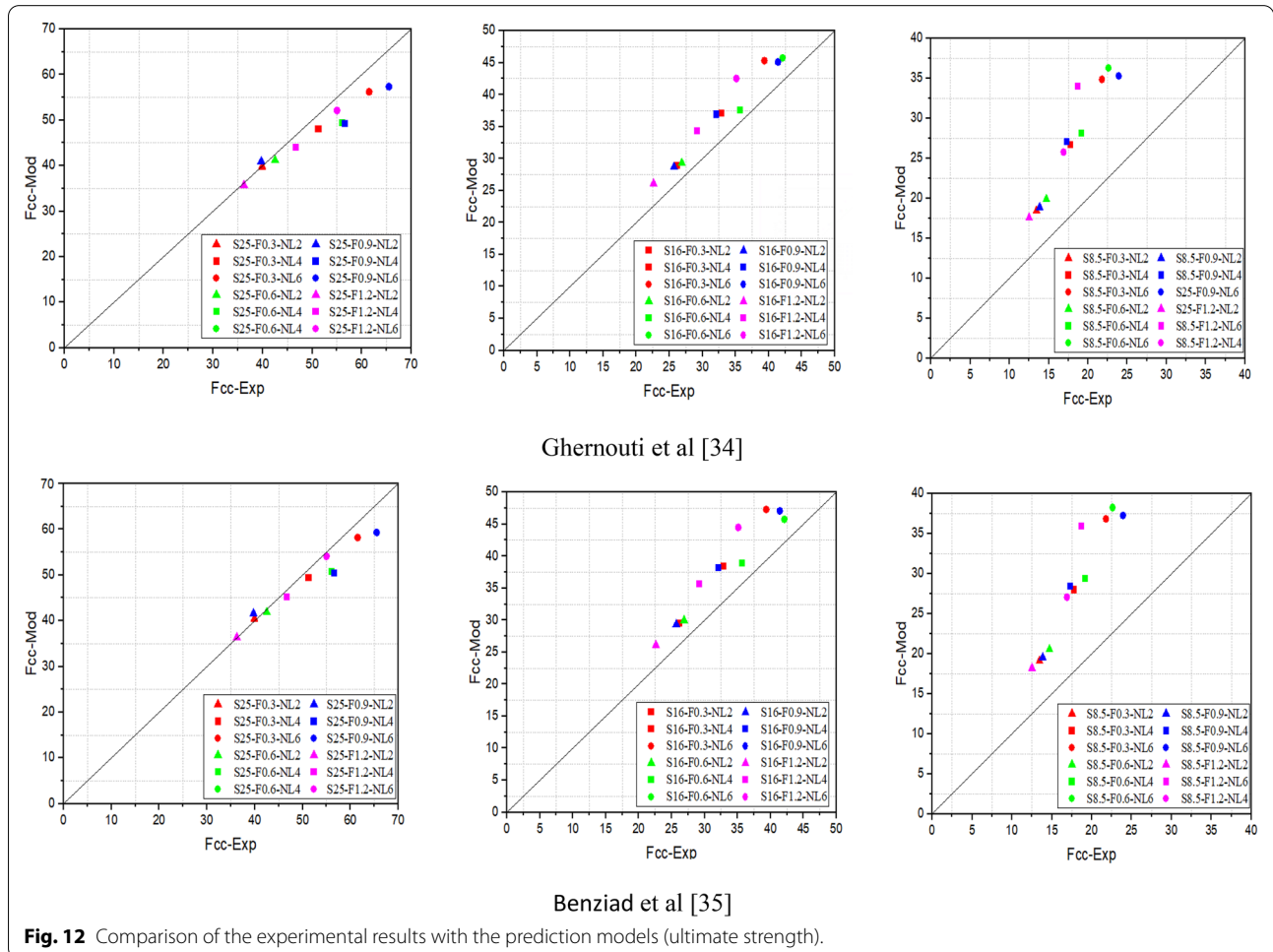


Fig. 12 Comparison of the experimental results with the prediction models (ultimate strength).

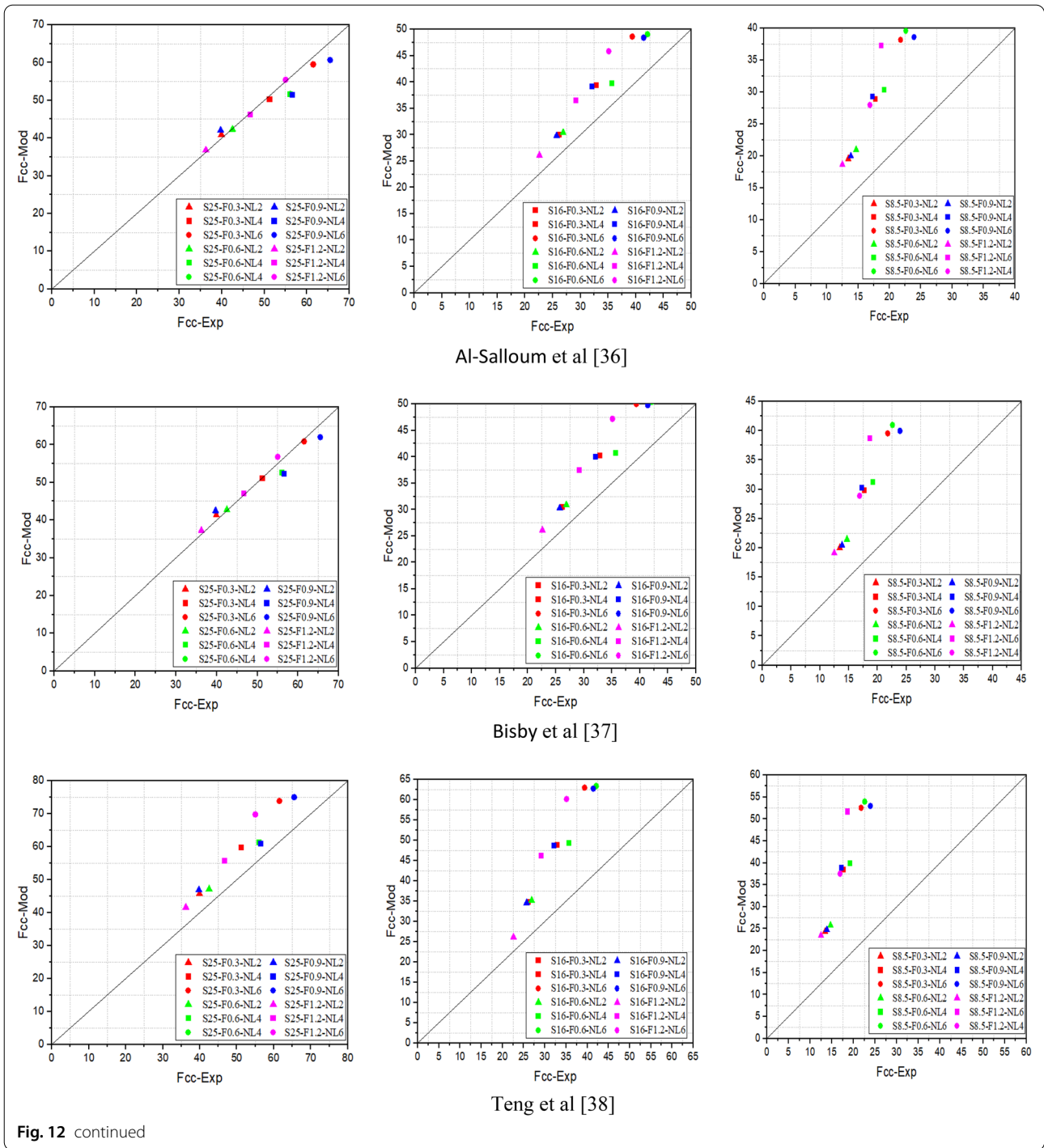


Fig. 12 continued

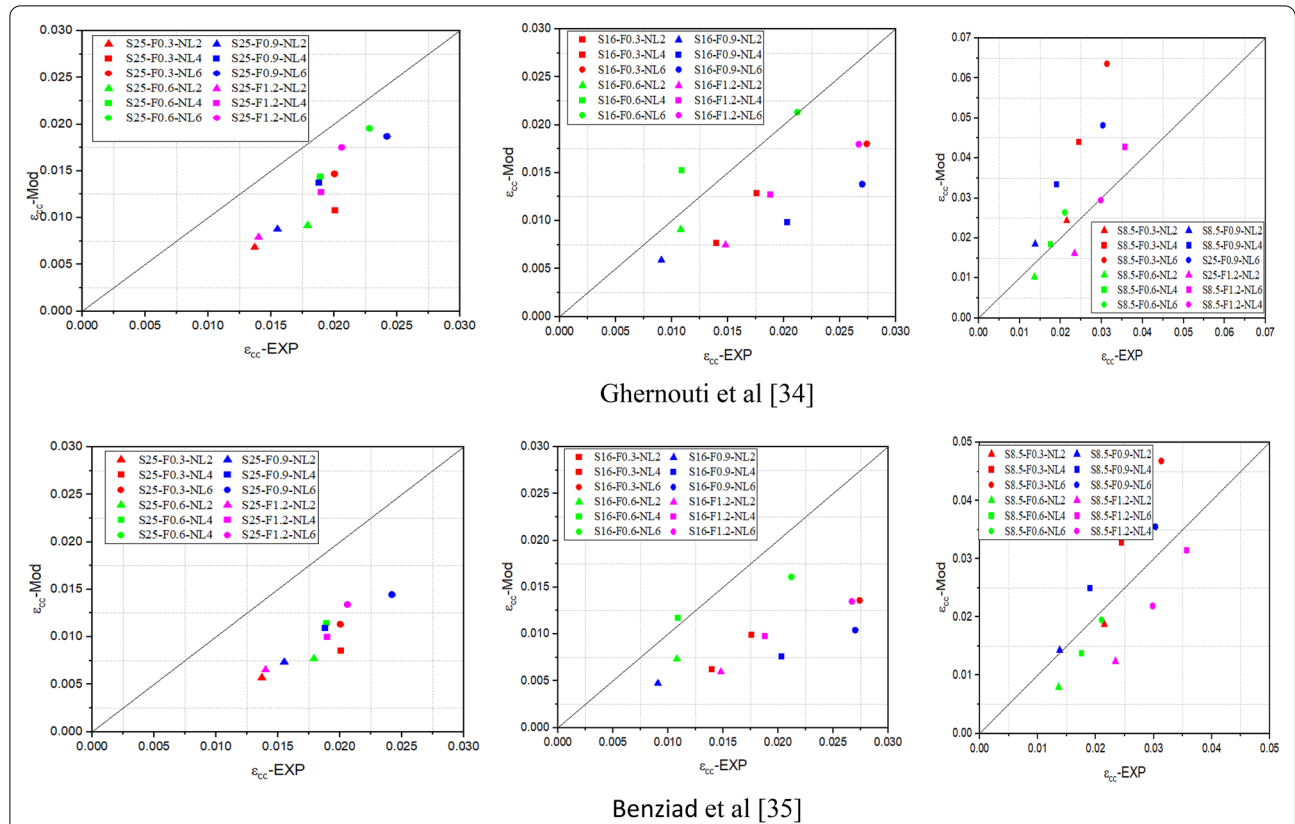


Fig. 13 Comparison of the experimental results with the prediction models (ultimate strain).

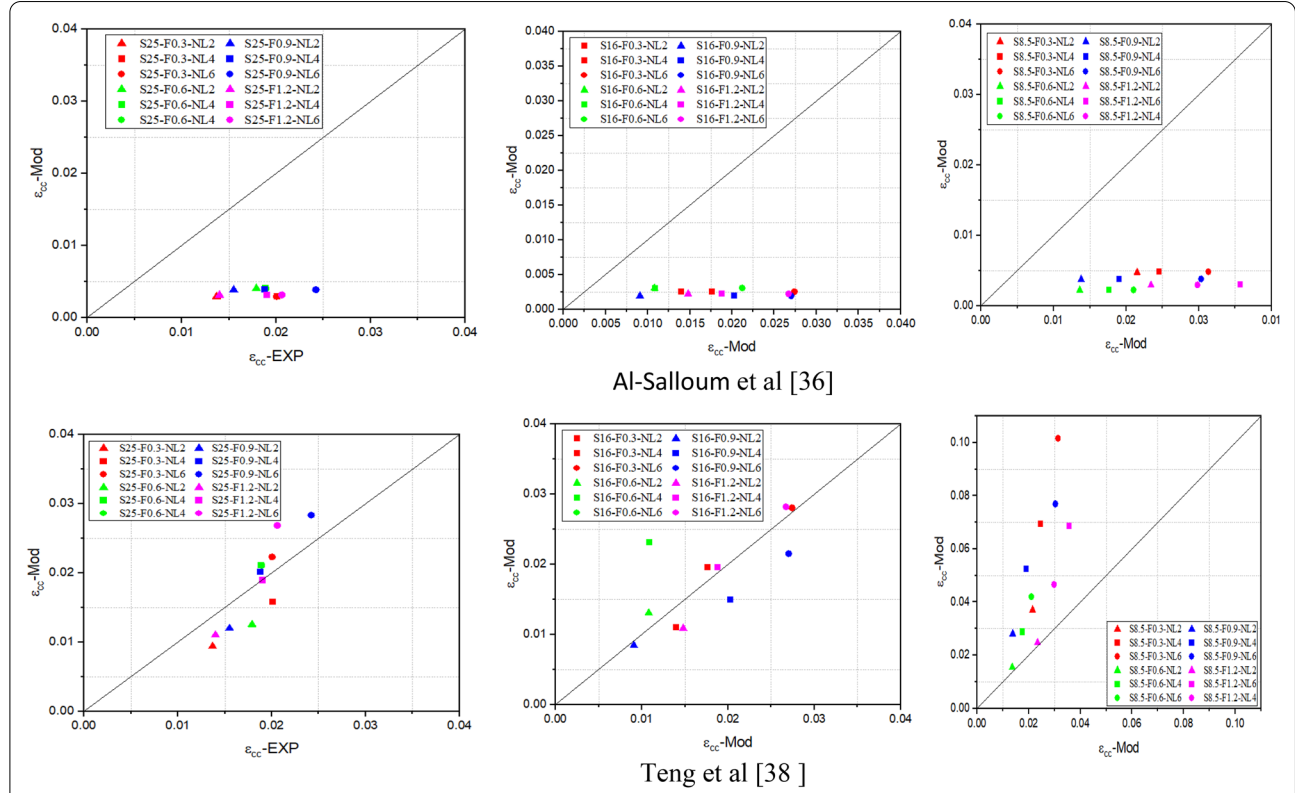


Fig. 13 continued

- The confinement effect of GFRP is relatively higher for concrete samples containing ARGF with a percentage equal to 0.6 wt.%.
- The theoretical predictions of models are close to the experimental results of high strength of GFCC but not close to the experimental results for low strength of GFCC. However, there is still a need to develop more accurate strength models for GFRP-confined GFCC.
- The current ultimate strain models are poor for accurately predicting the ultimate strain of the GFRP-confined GFCC.

Acknowledgements

Not applicable.

Authors' contributions

DY: conceptualization, methodology, investigation, validation, formal analysis, investigation, data curation, writing-original draft preparation, writing-review and editing, visualization; MS: investigation, formal analysis, data curation, writing-original draft preparation, writing-review and editing, visualization; TB: Proof reading, Formatting, Revise paper, Grammatical improvement. All authors read and approved the final manuscript.

Authors' information

Dr Yahiaoui Djarir is a lecturer at the department of Civil Engineering, University of Batna2, Algeria.

Dr Mohamed Saadi is a lecturer at the department of Civil Engineering, University of Batna2, Algeria.

Dr Tayeb Bouzid is a lecturer at the department of Civil Engineering, University of Batna2, Algeria.

Funding

Not applicable.

Received: 2 October 2021 Accepted: 6 April 2022

Published online: 19 July 2022

References

- Al-Salloum, Y. A. (2007). Compressive strength models of FRP-confined concrete. In: S.T. Smith (Ed.), Proceedings of the Asia-Pacific conference of FRP in structures (APFIS 2007), Hong Kong: University of Hong Kong, 2007, pp. 175–180.
- Bazli, M., Ashrafi, H., & Oskouei, A. V. (2016). Effect of harsh environments on mechanical properties of GFRP pultruded profiles. *Composites Part B Engineering*, 99, 203–215.
- Benzaïd, R., Mesbah, H., & Chikh, N. E. (2010). FRP-confined concrete cylinders: Axial compression experiments and strength model. *Journal of Reinforced Plastics and Composites*, 29(16), 2469–2488.
- Bisby, L. A., Dent, A. J., & Green, M. F. (2005). Comparison of confinement models for fiber-reinforced polymer-wrapped concrete. *ACI Structural Journal*, 102(1), 62–72.
- Chao, S. H., Naaman, A. E., & Parra-Montesinos, G. J. (2009). Bond behavior of reinforcing bars in tensile strain-hardening fiber reinforced cement composites. *ACI Structural Journal*, 106, 897–906.
- Christian, S. J., & Billington, S. L. (2011). Mechanical response of PHB- and cellulose acetate natural fiber-reinforced composites for construction applications. *Composites Part B Engineering*, 42(7), 1920–1928.
- Cromwell, J. R., Harries, K. A., & Shahrooz, B. M. (2011). Environmental durability of externally bonded FRP materials intended for repair of concrete structures. *Construction and Building Materials*, 25, 2528–2539.
- Feng, J. H., Su, Y. L., & Qian, C. X. (2019). Coupled effect of PP fiber, PVA fiber and bacteria on self-healing efficiency of early-age cracks in concrete. *Construction and Building Materials*. <https://doi.org/10.1016/j.conbuildmat.2019.116810>
- Feng, P., Wang, J., Wang, Y., Loughery, D., & Niu, D. (2014). Effects of corrosive environments on properties of pultruded GFRP plates. *Composites Part B Engineering*, 67, 427–433.
- Ganesan, N., Indira, P. V., & Sabeena, M. V. (2014). Bond stress slip response of bars embedded in hybrid fiber reinforced high performance concrete. *Construction and Building Materials*, 50, 108–115. <https://doi.org/10.1016/j.conbuildmat.2013.09.032>
- Ghernouti, Y., & Rabehi, B. (2011). FRP-confined short concrete columns under compressive loading: Experimental and modeling investigation. *Journal of Reinforced Plastics and Composites*, 30(3), 241–255.
- Guo, Y. H., Hu, X. Y., & Lv, J. F. (2019). Experimental study on the resistance of basalt fiber reinforced concrete to chloride penetration. *Construction and Building Materials*, 223, 142–155. <https://doi.org/10.1016/j.conbuildmat.2019.06.211>
- Kasagani, H., & Rao, C. B. K. (2018). Effect of graded fibers on stress strain behaviour of Glass Fiber Reinforced Concrete in tension. *Construction and Building Materials*, 183, 592–604. <https://doi.org/10.1016/j.conbuildmat.2018.06.193>
- Kizilkanat, A. B., Kabay, N., Akyüncü, V., Chowdhury, S., & Akça, A. H. (2015). Mechanical properties and fracture behavior of basalt and glass fiber reinforced concrete: An experimental study. *Construction and Building Materials*, 100, 218–224.
- Lam, L., & Teng, J. G. (2003). Design-oriented stress-strain model for FRP-confined concrete. *Construction and Building Materials*, 17, 471–489.
- Li, Y. L., Zhao, X. L., Raman Singh, R. K., & Al-Saadi, S. (2016). Experimental study on seawater and sea sand concrete filled GFRP and stainless steel tubular stub columns. *Thin-Walled Structures*, 106, 390–406.
- Liu, F. Y., Ding, W. Q., & Qiao, Y. F. (2020). Experimental investigation on the tensile behavior of hybrid steel-PVA fiber reinforced concrete containing fly ash and slag powder. *Construction and Building Materials*. <https://doi.org/10.1016/j.conbuildmat.2020.118000>
- Meda, A., Mostosi, S., Rinaldi, Z., & Riva, P. (2016). Corroded RC columns repair and strengthening with high-performance fiber-reinforced concrete jacket. *Materials and Structures*, 49, 1967–1978.
- Mirmiran, A., & Shahawy, M. (1997). Dilation characteristics of confined concrete. *Mech Cohesive-Frict Mater*, 2(3), 237–249.
- Mohammadhosseini, H., Tahir, M. M., Alaskar, A., Alabduljabbar, H., & Alyousef, R. (2020). Enhancement of strength and transport properties of a novel preplaced aggregate fiber reinforced concrete by adding waste polypropylene carpet fibers. *J Build Eng*. <https://doi.org/10.1016/j.jobbe.2019.101003>
- Niu, D. T., Su, L., Luo, Y., Huang, D. G., & Luo, D. M. (2020). Experimental study on mechanical properties and durability of basalt fiber reinforced coral aggregate concrete. *Construction and Building Materials*. <https://doi.org/10.1016/j.conbuildmat.2019.117628>
- Shaikh Ahmed, F. U. (2013). Review of mechanical properties of short fiber reinforced geopolymer composites. *Construction and Building Materials*, 43, 37–49.
- Signorini, C., Sola, A., Malchiodi, B., Nobili, A., & Gatto, A. (2020). Failure mechanism of silica coated polypropylene fibers for Fiber Reinforced Concrete (FRC). *Construction and Building Materials*. <https://doi.org/10.1016/j.conbuildmat.2019.117549>
- Spoelstra, M. R., & Monti, G. (1999). FRP-confined concrete model. *Journal of Composites for Construction*, 3(3), 143–150.
- Standards and literature references for composite materials—D638 (1990). 2nd Ed., ASTM, West Conshohocken, PA.
- Sun, X. J., Gao, Z., Cao, P., & Zhou, C. J. (2019). Mechanical properties tests and multiscale numerical simulations for basalt fiber reinforced concrete. *Construction and Building Materials*, 202, 58–72. <https://doi.org/10.1016/j.conbuildmat.2019.01.018>
- Tahsiri, H., Sedehi, O., Khaloo, A., & Raisi, E. M. (2015). Experimental study of RC jacketed and CFRP strengthened RC beams. *Construction and Building Materials*, 95, 476–485.
- Teng, J., Huang, Y. L., Lam, L., & Ye, L. P. (2007). Theoretical model for fiber-reinforced polymer-confined concrete. *Journal of Composites for Construction*, 11(2), 201–210.
- Wang, X. H., Zhang, S. R., Wang, C., Cao, K. L., Wei, P. Y., & Wang, J. X. (2019). Effect of steel fibers on the compressive and splitting-tensile behaviours of cellular concrete with millimeter-size pores. *Construction and Building Materials*, 221, 60–73. <https://doi.org/10.1016/j.conbuildmat.2019.06.069>

- Xie, J. H., Fang, C., Lu, Z. Y., Li, Z. J., & Li, L. J. (2019). Effects of the addition of silica fume and rubber particles on the compressive behaviour of recycled aggregate concrete with steel fibers. *Journal of Cleaner Production*, 197, 656–667. <https://doi.org/10.1016/j.jclepro.2018.06.237>
- Zheng, D., Song, W. D., Fu, J. X., Xue, G. L., Li, J. J., & Cao, S. A. (2020). Research on mechanical characteristics, fractal dimension and internal structure of fiber reinforced concrete under uniaxial compression. *Construction and Building Materials*. <https://doi.org/10.1016/j.conbuildmat.2020.120351>
- Zhu, D. J., Liu, S., Yao, Y. M., Li, G. S., Du, Y. X., & Shi, C. J. (2019). Effects of short fiber and pretension on the tensile behavior of basalt textile reinforced concrete. *Cement and Concrete Composites*, 96, 33–45. <https://doi.org/10.1016/j.cemconcomp.2018.11.015>

Publisher's Note

Springer Nature remains neutral with regard to jurisdictional claims in published maps and institutional affiliations.

Submit your manuscript to a SpringerOpen[®] journal and benefit from:

- ▶ Convenient online submission
- ▶ Rigorous peer review
- ▶ Open access: articles freely available online
- ▶ High visibility within the field
- ▶ Retaining the copyright to your article

Submit your next manuscript at ▶ [springeropen.com](https://www.springeropen.com)
